J|A|C|S ARTICLES

Published on Web 04/02/2009

Expanding the Peptide β-Turn in $\alpha\gamma$ Hybrid Sequences: 12 Atom Hydrogen Bonded Helical and Hairpin Turns

Sunanda Chatterjee,[†] Prema G. Vasudev,[‡] Srinivasarao Raghothama,[§] Chandrasekharan Ramakrishnan,[†] Narayanaswamy Shamala,*[,‡] and Padmanabhan Balaram*[,†]

Molecular Biophysics Unit, Department of Physics, and NMR Research Centre, Indian Institute of Science, Bangalore-560012, India

Received January 26, 2009; E-mail: pb@mbu.iisc.ernet.in; shamala@physics.iisc.ernet.in

Abstract: Hybrid peptide segments containing contiguous α and γ amino acid residues can form C_{12} hydrogen bonded turns which may be considered as backbone expanded analogues of C_{10} (β-turns) found in $\alpha\alpha$ segments. Exploration of the regular hydrogen bonded conformations accessible for hybrid $\alpha\gamma$ sequences is facilitated by the use of a stereochemically constrained γ amino acid residue gabapentin (1-aminomethylcyclohexaneacetic acid, Gpn), in which the two torsion angles about $C^{\gamma}-C^{\beta}$ (θ_1) and $C^{\beta}-C^{\alpha}$ (θ_2) are predominantly restricted to *gauche* conformations. The crystal structures of the octapeptides Boc-Gpn-Aib-Gpn-Aib-Gpn-Aib-Gpn-Aib-OMe (**1**) and Boc-Leu-Phe-Val-Aib-Gpn-Leu-Phe-Val-OMe (**2**) reveal two distinct conformations for the Aib-Gpn segment. Peptide **1** forms a continuous helix over the Aib(2)-Aib(6) segment, while the peptide **2** forms a β-hairpin structure stabilized by four cross-strand hydrogen bonds with the Aib-Gpn segment forming a nonhelical C_{12} turn. The robustness of the helix in peptide **1** in solution is demonstrated by NMR methods. Peptide **2** is conformationally fragile in solution with evidence of β-hairpin conformations being obtained in methanol. Theoretical calculations permit delineation of the various C_{12} hydrogen bonded structures which are energetically feasible in $\alpha\gamma$ and $\gamma\alpha$ sequences.

Introduction

Hybrid polypeptide sequences in which backbone homologated amino acids are interspersed with α amino acids provide entry to new classes of foldamer structures.[1] The insertion of β, γ, and δ amino acids into α amino acid containing sequences has been investigated by several groups in recent years.[2] This upsurge of interest in the conformational properties of the homologated amino acid residues has been catalyzed by the observation of novel hydrogen bonded structures in homo oligopeptides containing β and γ amino acid residues. The groups of Seebach and Gellman demonstrated that the structures in which the hydrogen bond directionality runs opposite to that in canonical α peptide helices are accessible in homo oligo β-peptides.[1,3] The insertion of homologated residues also confers proteolytic stability to the peptide backbone providing entry to practically useful, stable analogues of medicinally important sequences.[1a,4] While backbone homologation enhances the range of available conformations, β and γ residues have been found to be readily accommodated into the regular structures formed by α peptides, helices, hairpins, and hydrogen bonded turns.[5] Exploration of the range of folded structures accessible to backbone homologated residues is facilitated by the use of conformationally constrained model amino acids. Backbone conformational restriction may be introduced by cyclization, as in the case of β amino acids derived from 2-aminocyclopentane carboxylic acid and 2-aminocyclohexane carboxylic acid.[3b−d] Alternatively, the introduction of geminal substituents at one of the backbone carbon atoms can be used to restrict torsional freedom, in a manner analogous to the C^{α} tetrasubstituted α

[†] Molecular Biophysics Unit.
[‡] Department of Physics.
[§] NMR Research Centre.

(1) For reviews, see:(a) Seebach, D.; Beck, A. K.; Bierbaum, D. J. *Chem. Biodiversity* **2004**, *1*, 1111–1239. (b) Cheng, R. P.; Gellman, S. H.; DeGrado, W. F. *Chem. Rev.* **2001**, *101*, 3219–3232. (c) Goodman, C. M.; Choi, S.; Shandler, S.; DeGrado, W. F. *Nat. Chem. Biol.* **2007**, *3*, 252–262. (d) Gellman, S. H. *Acc. Chem. Res.* **1998**, *31*, 173–180. (e) Horne, W. S.; Gellman, S. H. *Acc. Chem. Res.* **2008**, *41*, 1399–1408.

(2) For representative references, see:(a) Roy, R. S.; Balaram, P. *J. Peptide Res.* **2004**, *63*, 279–289. (b) Chatterjee, S.; Roy, R. S.; Balaram, P. *J. R. Soc. Interface* **2006**, *4*, 587–606. (c) Choi, S. H.; Guzei, I. A.; Gellman, S. H. *J. Am. Chem. Soc.* **2007**, *129*, 13780–13781. (d) Horne, W. S.; Price, J. L.; Keck, J. L.; Gellman, S. H. *J. Am. Chem. Soc.* **2007**, *129*, 4178–4180. (e) De Pol, S.; Zorn, C.; Klein, C. D.; Zerbe, O.; Reiser, O. *Angew. Chem., Int. Ed.* **2004**, *43*, 511–514. (f) Seebach, D.; Jaun, B.; Sebesta, R.; Mathad, R. I.; Flogel, O.; Limbach, M.; Sellner, H.; Cottens, S. *Helv. Chim. Acta* **2006**, *89*, 1801–1825. (g) Srinivasulu, G.; Kumar, S. K.; Sharma, G. V. M.; Kunwar, A. C. *J. Org. Chem.* **2006**, *71*, 8395–8400. (h) Baldauf, C.; Gunther, R.; Hofmann, H. J. *Biopolymers* **2006**, *84*, 408–413. (i) Baldauf, C.; Gunther, R.; Hofmann, H. J. *J. Org. Chem.* **2006**, *71*, 1200–1208.

(3) (a) Seebach, D.; Overhand, M.; Kühnle, F. N. M.; Martinoni, B. *Helv. Chim. Acta* **1996**, *79*, 913–941. (b) Appella, D. H.; Christianson, L. A.; Karle, I. L.; Powell, D. R.; Gellman, S. H. *J. Am. Chem. Soc.* **1996**, *118*, 13071–13072. (c) Appella, D. H.; Christianson, L. A.; Klein, D. A.; Powell, D. R.; Huang, X.; Barchi, J. J., Jr.; Gellman, S. H. *Nature (London)* **1997**, *387*, 381–384. (d) Appella, D. H.; Christianson, L. A.; Klein, D. A.; Richards, M. R.; Powell, D. R.; Gellman, S. H. *J. Am. Chem. Soc.* **1999**, *121*, 7574–7581.

(4) (a) Seebach, D.; Gardiner, J. *Acc. Chem. Res.*, **2008**, *41*, 1366–1375. (b) Schmitt, M. A.; Weisblum, B.; Gellman, S. H. *J. Am. Chem. Soc.* **2007**, *129*, 417–428. (c) Stephens, O.; Kim, S.; Welch, B. D.; Hodsdon, M. E.; Kay, M. S.; Schepartz, A. *J. Am. Chem. Soc.* **2005**, *127*, 13126–13127. (d) Kritzer, J. S.; Stephens, O. M.; Guarracino, D. A.; Reznik, S. K.; Schepartz, A. *Bioorg. Med. Chem.* **2005**, *13*, 11–16.

 10.1021/ja900618h CCC: $40.75

residue, α-aminoisobutyric acid (Aib).[6] This approach is exemplified by the conformational studies on peptides containing the substituted β residue βAc_6c (1-aminocyclohexaneacetic acid)[7] and the γ residue analog gabapentin (1-aminomethylcyclohexaneacetic acid, Gpn). Positioning of the cyclohexyl group at the C^{β} carbon atom in Gpn restricts the $C^{\gamma}-C^{\beta}$ (θ_1) and $C^{\beta}-C^{\alpha}$ (θ_2) torsion angles with the *gauche*−*gauche* conformation being overwhelmingly preferred.[8] In this report we present two distinctly different oligopeptide structures which possess C_{12} hydrogen bonded $\alpha\gamma$ turns, which may be considered as backbone expanded analogues of the widely characterized C_{10} hydrogen bonded β-turn in αα segments.[9a] Crystal structures of the octapeptides Boc-Gpn-Aib-Gpn-Aib-Gpn-Aib-Gpn-Aib-OMe (**1**) and Boc Leu-Phe-Val-Aib-Gpn-Leu-Phe-Val-OMe (**2**) reveal that **1** adopts an almost complete C_{12} helical conformation, while **2** adopts a β-hairpin structure promoted by a centrally positioned Aib-Gpn $\alpha\gamma$ C_{12} turn. These two structures provide a definitive characterization of an $\alpha\gamma$ segment in two distinctly different secondary structures. The stability of these structures in solution in organic solvents is demonstrated by NMR methods. Theoretical conformational analysis employing methods analogous to those used in delineation of hydrogen bonded β-turns in αα segments[9] permits identification of accessible C_{12} turns in $\alpha\gamma$ segments.

Experimental Procedures

Peptide Synthesis. Peptides were synthesized by conventional solution phase methods using a fragment condensation strategy. The *tert*-butyloxycarbonyl group (Boc) was used for N-terminal protection, and the C-terminal was protected as a methyl ester (OMe). Deprotection at the N-terminus was performed using 98% formic acid, and saponification was done to remove the C-terminal protecting groups. Couplings were mediated by *N*,*N*′-dicyclohexylcarbodiimide/1-hydroxybenzotriazole (DCC/HOBt)[10] (see Supporting Information for details of procedures used). Several intermediates were characterized by 400 MHz ^{1}H NMR spectra and by mass spectrometry and were used without further purification. The target peptides were purified over medium pressure liquid chromatography (MPLC) on a C_{18} column (particle 40−63 μ; column dimension 230 mm × 26 mm) using water−methanol gradients (50−100%) and HPLC (C_{18}, 5−10 μ, column dimension 9.4 mm × 25 cm) employing water−methanol gradients (50−100%), using detection at 226 nm. The purified peptides were characterized by electrospray ionization mass spectrometry (ESI-MS) and by assignment of the 500 MHz ^{1}H spectra.

Crystal Structure Determination. The crystals of peptide **1** were readily obtained from a solution in methanol/water. Crystals of peptide **2** were difficult to obtain from common crystallization solvents like methanol/water, ethyl acetate/petroleum ether, and isopropanol/water, which always yielded thin fibers or white precipitates. Crystallization of the peptide from a 1:1 mixture of methanol and dioxane in the presence of small amounts of water yielded a single crystal suitable for X-ray data collection.

X-ray intensity data were collected at room temperature using Mo Kα ($\lambda = 0.710\ 73$ Å) radiation for both of the peptide crystals. A combination of ω and ϕ scans were performed to collect the data for peptide **1**, mounted on a Bruker AXS KAPPA APEX II CCD diffractometer. The data for peptide **2** were collected on a Bruker AXS SMART APEX CCD diffractometer using the ω scan. The data for peptide **2** were obtained up to a resolution of 1.1 Å. Peptide **1** crystallized in the monoclinic, centrosymmetric space group $P2_1/n$, while peptide **2** crystallized in the orthorhombic space group $P2_12_12_1$. The unit cell dimensions are as follows: Peptide **1**, $a = 11.961$ Å, $b = 18.513$ Å, $c = 29.497$ Å, $\beta = 92.78°$, and $V = 6524.4$ Å^3 and Peptide **2**, $a = 9.558$ Å, $b = 26.278$ Å, $c = 27.434$ Å, $V = 6890$ Å^3. The structures of both the peptides were obtained by direct methods using SHELXD[11] and were refined against F^2 with full-matrix least-squares methods in SHELXL-97.[12] The residual peaks obtained after the anisotropic refinement of nonhydrogen atoms of peptide **2** could be best modeled as tetrahydrofuran (THF), a contaminant in the solvent, which might have been trapped in the crystal. All the hydrogen atoms were fixed in idealized positions and were refined as riding over the carbon or nitrogen atoms to which they are bonded, in the final cycles of refinement. In the case of peptide **2**, restraints were applied to bond lengths and bond angles of the side chains of Phe(2) and Leu(6) residues and for the solvent molecule. The final *R*-factor obtained for peptide **1** is 7.3% ($wR_2 = 15.7\%$) for 2692 observed data [$F_o > 4\sigma(F)$] and 722 parameters. The *R*-factor obtained for peptide **2** is 12.3% ($wR_2 = 29.5\%$) for 2537 observed reflections [$F_o > 4\sigma(F)$] and 748 parameters (Supporting Information, Table S1).

Theoretical Conformational Analysis. The sterically allowed conformations for C_{12} hydrogen bonded structures were computed using model peptides Ac-Gly-γAbu-NHMe (for $\alpha\gamma$ segments) and Ac-γAbu-Gly-NHMe (for $\gamma\alpha$ segments). The standard values of internal parameters were used for model building.[13] The bond angles and bond lengths for the models used are provided as Supporting Information (Figure S11). The backbone torsion angles ϕ, ψ for the α residue and ϕ, θ_1, θ_2, ψ for the γ residue were systematically varied. The values of θ_1 and θ_2 were varied 30° around the nine possible combinations of θ_1 (deg) and θ_2 (deg) (60, 60; 60, −60, 60, 180; 180, 60; four enantiomeric combinations and 180, 180), at 5° intervals. In each case the values of ϕ and ψ for the α- and γ-residues were varied from −180° to +180° at 20° intervals. The

(5) Helices:(a) Karle, I. L.; Pramanik, A.; Banerjee, A.; Battacharjya, S.; Balaram, P. *J. Am. Chem. Soc.* **1997**, *119*, 9087–9095. (b) Roy, R. S.; Karle, I. L.; Raghothama, S.; Balaram, P. *Proc. Natl. Acad. Sci. U.S.A.* **2004**, *101*, 16478–16482. (c) Ananda, K.; Vasudev, P. G.; Sengupta, A.; Raja, K. M. P.; Shamala, N.; Balaram, P. *J. Am. Chem. Soc.* **2005**, *127*, 16668–16674. (d) Choi, S. H.; Guzei, I. A.; Spencer, L. C.; Gellman, S. H. *J. Am. Chem. Soc.* **2008**, *130*, 6544–6550β-hairpins: (e) Karle, I. L.; Gopi, H. N.; Balaram, P. *Proc. Natl. Acad. Sci. U.S.A.* **2002**, *99*, 5160–5164. (f) Karle, I. L.; Gopi, H. N; Balaram, P. *Proc. Natl. Acad. Sci. U.S.A.* **2001**, *98*, 3716–3719. (g) Roy, R. S.; Gopi, H. N.; Raghothama, S.; Karle, I. L.; Balaram, P. *Chem.*−*Eur. J.* **2006**, *12*, 3295–3302. (h) Rai, R.; Vasudev, P. G.; Ananda, K.; Raghothama, S.; Shamala, N.; Karle, I. L.; Balaram, P. *Chem.*−*Eur. J.* **2007**, *13*, 5917–5926.

(6) (a) Prasad, B. V. V.; Balaram, P. *CRC Crit. Rev. Biochem.* **1984**, *16*, 307–347. (b) Karle, I. L.; Balaram, P. *Biochemistry* **1990**, *29*, 6747–6756. (c) Aravinda, S.; Shamala, N.; Roy, R. S.; Balaram, P. *Proc. Indian Acad. Sci. (Chem. Sci.)* **2003**, *115*, 373–400. (d) Toniolo, C.; Benedetti, E. *Macromolecules* **1991**, *24*, 4004–4009. (e) Crisma, M.; Formaggio, F.; Toniolo, C.; Moretto, A. *Biopolymers (Peptide Sci.)* **2006**, *84*, 3–12. (f) Bolin, K. A.; Millhauser, G. L. *Acc. Chem. Res.* **1999**, *32*, 1027–1033. (g) Marshall, G. R.; Bosshard, H. E. *Circ. Res.* **1972**, *30/31*, 143.

(7) (a) Seebach, D.; Abele, S.; Sifferlen, T.; Hänggi, M.; Gruner, S.; Seiler, P. *Helv. Chim. Acta* **1998**, *81*, 2218–2243. (b) Vasudev, P. G.; Rai, R.; Shamala, N.; Balaram, P. *Biopolymers (Pept. Sci.)* **2008**, *90*, 138–150.

(8) (a) Ananda, K.; Aravinda, S.; Vasudev, P. G.; Raja, K. M. P.; Sivaramakrishnan, H.; Nagarajan, K.; Shamala, N.; Balaram, P. *Curr. Sci.* **2003**, *85*, 1002–1011. (b) Vasudev, P. G.; Ananda, K.; Chatterjee, S.; Aravinda, S.; Shamala, N.; Balaram, P. *J. Am. Chem. Soc.* **2007**, *129*, 4039–4048. (c) Chatterjee, S.; Vasudev, P. G.; Ananda, K.; Raghothama, S.; Shamala, N.; Balaram, P. *J. Org. Chem.* **2008**, *73*, 6595–6606. (d) Vasudev, P. G.; Chatterjee, S.; Ananda, K.; Shamala, N. *Angew. Chem., Int. Ed.* **2008**, *47*, 6430–6432.

(9) (a) Venkatachalam, C. M. *Biopolymers* **1968**, *6*, 1425–1436. (b) Ramachandran, G. N.; Sasisekharan, V. *Adv. Protein Chem.* **1968**, *23*, 284–438. (c) Paul, P. K. C.; Ramakrishnan, C. *J. Biomol. Struct. Dyn.* **1985**, *2*, 879–898.

(10) Schneider, T. R.; Sheldrick, G. M. *Acta Crystallogr.* **2002**, *D58*, 1772–1779.

(11) *Peptides: Synthesis, structure and applications*; Gutte, B., Ed.; Academic Press: New York, 1995.

(12) Sheldrick, G. M. *SHELXL-97, A program for crystal structure refinement*; University of Göttingen: Göttingen, 1997.

(13) Corey, R. B.; Pauling, L. *Proc. R. Soc. London* **1953**, *B141*, 10–20.

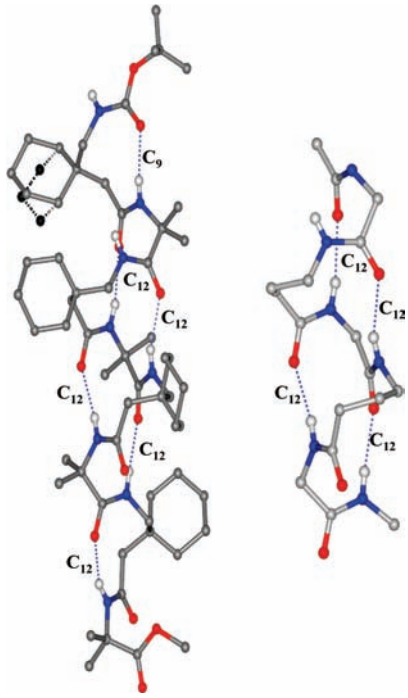

Figure 1. Molecular conformation of peptide **1** determined in crystals. The backbone of the C_{12} helical segment is shown separately (right).

conformations which satisfied the criteria of formation of a hydrogen bond (N···O between 2.6−3.3 Å, H−N···O < 40°) were further subjected to a steric check.[9b] The torsion angle combinations with $\theta_2 = \pm 60°$, $\theta_1 = 180°$ (only for $\alpha\gamma$ case) and $\theta_1 = \pm 60°$, $\theta_2 = 180°$ (only for $\gamma\alpha$ case) and $\theta_1 = \theta_2 = 180°$ (for both $\alpha\gamma$ and $\gamma\alpha$ cases) failed to satisfy the steric/hydrogen bond criteria and were discarded. Conformational energies were computed using the potential functions described earlier.[9b] Only nonbonded Buckingham 6-exp potentials and hydrogen bond energies were computed. The electrostatic and torsional functions make a very minor contribution to the total energy. All the programs needed for this analysis were written in FORTRAN. The backbone torsion angles and energy for unique classes of conformations of $\alpha\gamma$ and $\gamma\alpha$ segments, resulting from this calculation, are provided as Supporting Information. Unique sets of conformations obtained from these calculations were rebuilt using INSIGHT-II. These were subjected to 100 cycles of minimization to optimize the hydrogen bonds using the CVFF force field in the DISCOVER module.

Results and Discussion

Solid State Conformations of Peptides 1 and 2. Molecular conformations of the peptides Boc-Gpn-Aib-Gpn-Aib-Gpn-Aib-Gpn-Aib-OMe (**1**) and Boc-Leu-Phe-Val-Aib-Gpn-Leu-Phe-Val-OMe (**2**) determined in crystals are shown in Figures 1 and 2. The relevant backbone torsion angles and hydrogen bond parameters are summarized in Tables 1 and 2, respectively. The alternating Gpn-Aib oligomer (**1**) adopts a continuous helical conformation stabilized by six intramolecular hydrogen bonds. The central segment Aib(2)-Aib(6) forms an almost perfect $\alpha\gamma$ C_{12} helix, which can be formally considered as a backbone expanded analogue of the C_{10}-helix (3_{10}- helix) observed in all α sequences.[15] All four Aib residues adopt helical conformations with the sole difference that the terminal residue Aib(8) has the opposite hand, a feature commonly observed in Aib peptides.[16] All Gpn residues adopt conformations in which the torsion angles θ_1 and θ_2 are *gauche*, with a reversal of sign being observed at the C-terminal Gpn(7) residue. In crystals, the columns of helices related by the n-glide symmetry show a slippage of helices along the direction of the helix axis, which places the two donor groups NH(1) and NH(3) perfectly in hydrogen bonding position to acceptor groups CO(5) and CO(7) of two other helices (Figure S2, Supporting Information). The chiral reversal of the helix at the penultimate Gpn(7) residue, rather than at the terminal Aib(8) residue, avoids steric hindrance in such a packing arrangement. The Gpn(1) and the Gpn(7) residues, which flank the central C_{12} helical segment, adopt C_9 hydrogen bonded conformations that have been found to be highly favored in short peptides containing this residue.[8b] The C_9 hydrogen bond formed by the γ-amino acid residue is the backbone expanded analogue of the C_7 (γ-turn) hydrogen bond formed by α-amino acids. Inspection of backbone torsion angles in Table 1 shows that the Gpn backbone conformations are similar in the C_9 and C_{12} hydrogen bonded structures. It should be noted that peptide **1** is an achiral structure crystallizing in a centrosymmetric space group and that molecules containing both senses of helical twist are present in the unit cell. The signs of torsion angles present in Table 1 correspond to one sense of twist. The four cyclohexyl rings that project outward adopt different conformations. While the cyclohexyl ring in Gpn(1) is disordered (refined with an occupancy of 0.8 for aminomethyl axial orientation and occupancy of 0.2 for the aminomethyl equatorial orientation), the rings of Gpn(3) and Gpn(5) have the aminomethyl group equatorial, while in Gpn(7) an axial orientation is observed.

Peptide **2** adopts an almost perfect β-hairpin conformation, stabilized by four interstrand hydrogen bonds between the two Leu-Phe-Val tripeptide segments. The central Aib(4)-Gpn(5) segment forms the C_{12} hydrogen bonded turn, which results in the reversal of polypeptide chain direction. The edge on view shown in Figure 2 illustrates the disposition of the side chains and the proximity of the facing Phe residues at positions 2 and 7. The torsion angles in Table 1 reveal dramatic differences between the values observed for the $\alpha\gamma$ turn in the C_{12} helix in peptide **1** and the $\alpha\gamma$ turn observed in the hairpin in peptide **2**. The Gpn(5) residue adopts an unusual conformation in which $\theta_2(C^\beta-C^\alpha)$ is almost fully extended (−167°). The aminomethyl group is now observed in an axial orientation with respect to the cyclohexyl ring. All six strand residues adopt the anticipated extended conformations, while Aib(4) adopts a right handed helical α_R conformation. The crystal structure of peptide **2** contains a single molecule of the solvent tetrahydrofuran (THF) which makes nonbonded contacts with the neighboring peptide molecules. Stereoviews of the molecular conformations and packing diagrams of peptides **1** and **2** are shown in the Supporting Information (Figures S1−S4).

The structures of peptides **1** and **2** illustrate two distinct hydrogen bonded turns formed by the Aib-Gpn, $\alpha\gamma$ segment. The robustness of the structures described above in solution is established by NMR methods.

Solution Conformations of Peptides 1 and 2. The 500 MHz spectrum of **1** revealed a completely dispersed set of eight NH resonances (Figure 3). The ROESY spectrum shown in Figure 3 reveals a complete set of sequential $N_iH-N_{i+1}H$ (d_{NN}) NOEs.

(14) Ramachandran, G. N.; Ramakrishnan, C.; Sasisekharan, V. *J. Mol. Biol.* **1963**, *7*, 95–99.
(15) (a) Donohue, J. *Proc. Natl. Acad. Sci. U.S.A.* **1953**, *39*, 470–478. (b) Toniolo, C.; Benedetti, E. *Trends Biochem. Sci.* **1991**, *16*, 350–353.
(16) Aravinda, S.; Shamala, N.; Balaram, P. *Chem. Biodiversity* **2008**, *5*, 1238–1262.

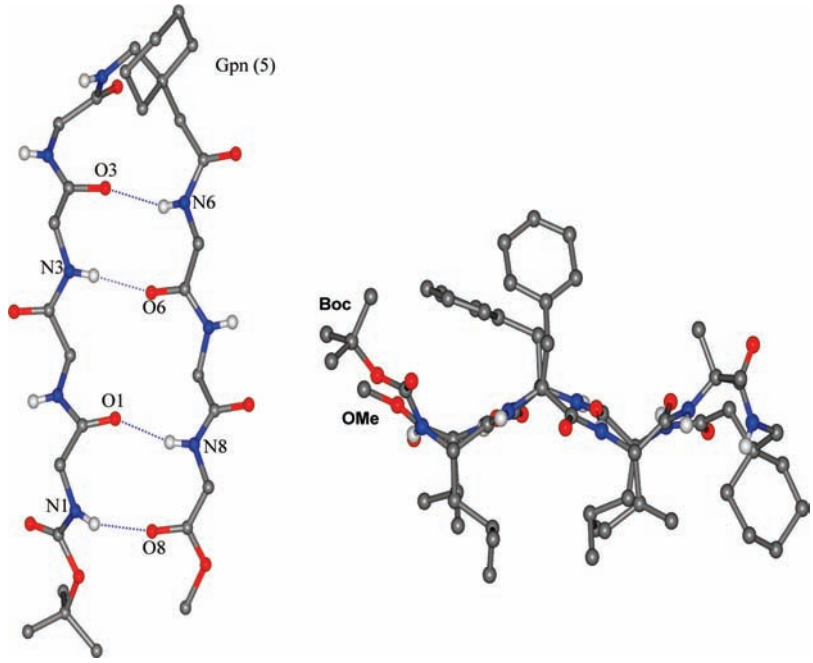

Figure 2. β-hairpin conformations of peptide **2** determined in crystals (left). For α residues, only the backbone atoms are shown, for clarity. Side view of the peptide β-hairpin, illustrating the pleated sheet formation and the orientations of side chains (right).

Table 1. Backbone Torsion Angles[a] for Peptides **1** and **2**

residue	ϕ	θ_1	θ_2	ψ	ω	Orientation of aminomethyl group
			Peptide **1**			
Gpn(1)	−120.0	62.3	73.7	−83.8	−167.4	disordered ring[b]
Aib(2)	−60.3			−40.7	−174.6	
Gpn(3)	−128.7	58.1	57.4	−111.3	−173.8	equatorial
Aib(4)	−55.9			−43.8	−169.7	
Gpn(5)	−126.1	50.4	63.1	−117.4	−171.8	equatorial
Aib(6)	−53.3			−42.8	177.9	
Gpn(7)	106.3	−68.9	−76.1	95.1	−174.9	axial
Aib(8)	58.3			33.5	176.7	
			Peptide **2**			
Leu(1)	−89			126	−178	
Phe(2)	−125			121	174	
Val(3)	−117			134	−173	
Aib(4)	−49			−41	−179	
Gpn(5)	−103	65	−167	104	−167	axial
Leu(6)	−146			141	156	
Phe(7)	−132			139	168	
Val(8)	−144			131	179	

[a] Esd's for torsion angles are approximately 0.7° (peptide **1**) and 2° (peptide **2**) [b] $a_N/e_N = 0.8{:}0.2$

Table 2. Hydrogen Bond Parameters in Peptides **1** and **2**

type	donor (D)	acceptor (A)	N···O (Å)	H···O (Å)	N−H···O (deg)
		Peptide **1**			
Intramolecular					
C_9	N2	O0	2.962	2.105	174.0
C_{12}	N4	O1	3.008	2.164	166.6
C_{12}	N5	O2	2.910	2.089	159.6
C_{12}	N6	O3	2.944	2.092	170.7
C_{12}	N7	O4	2.937	2.081	173.4
C_9	N8	O6	2.896	2.079	158.3
Intermolecular					
	N1	O5[a]	2.847	2.090	146.4
	N3	O7[b]	2.878	2.375	117.8
		Peptide **2**			
Intramolecular					
	N1	O8	2.897	2.111	152.0
	N3	O6	2.918	2.066	170.9
	N6	O3	3.080	2.268	157.4
	N8	O1	2.984	2.155	161.7
Intermolecular					
	N2	O7[c]	2.842	1.990	170.7
	N4	O5[c]	2.955	2.141	158.0
	N7	O2[d]	2.885	2.047	164.5

[a] Symmetry related by $x + {}^1/_2, -y - {}^1/_2, z + {}^1/_2$. [b] Symmetry related by $x - {}^1/_2, -y - {}^1/_2, z + {}^1/_2$. [c] Symmetry related by $x - 1, y, z$. [d] Symmetry related by $x + 1, y, z$.

The ROESY intensities show an alternating pattern of weak and strong NOEs. The d_{NN} NOEs across the Aib residue are stronger, while those across the Gpn residues are weaker. This is fully consistent with the conformation observed in crystals over the segment Aib(2)-Aib(6), in which d_{NN} Gpn ≈ 3.6 Å and d_{NN} Aib ≈ 2.8 Å. In the solid state conformation, the d_{NN} distances across the Gpn(1) and Gpn(7) residues are somewhat longer, 3.9 and 4.3 Å, respectively. The solvent exposure of the NH groups was probed by addition of the hydrogen bonding solvent DMSO-d_6 to a $CDCl_3$ solution of the peptide. The solvent titration curves shown in Figure 4 establish that only Gpn(1) NH shows an appreciable solvent shift. The NH resonances of Aib(2), Aib(4), Gpn(5), Aib(6), and Aib(8) show almost no solvent dependence, while a small downfield shift is evident for Gpn(3) NH (Supporting Information, Table S2). In the solid state conformation, the C_9 hydrogen bonded structure adopted at Gpn(1) results in the absence of any hydrogen bond interaction involving Gpn(3) NH. A greater degree of solvent sensitivity may have been anticipated for the Gpn(3) NH proton. Inspection of a space filling model (Figure 4) of the solid state conformation of peptide **1** reveals that the Gpn(3) NH is sterically shielded from the approach of solvent molecules by the neighboring cyclohexyl groups of Gpn(1) and Gpn(3) residues. The NMR results are thus consistent with a solution conformation which closely resembles that observed in the crystalline state.

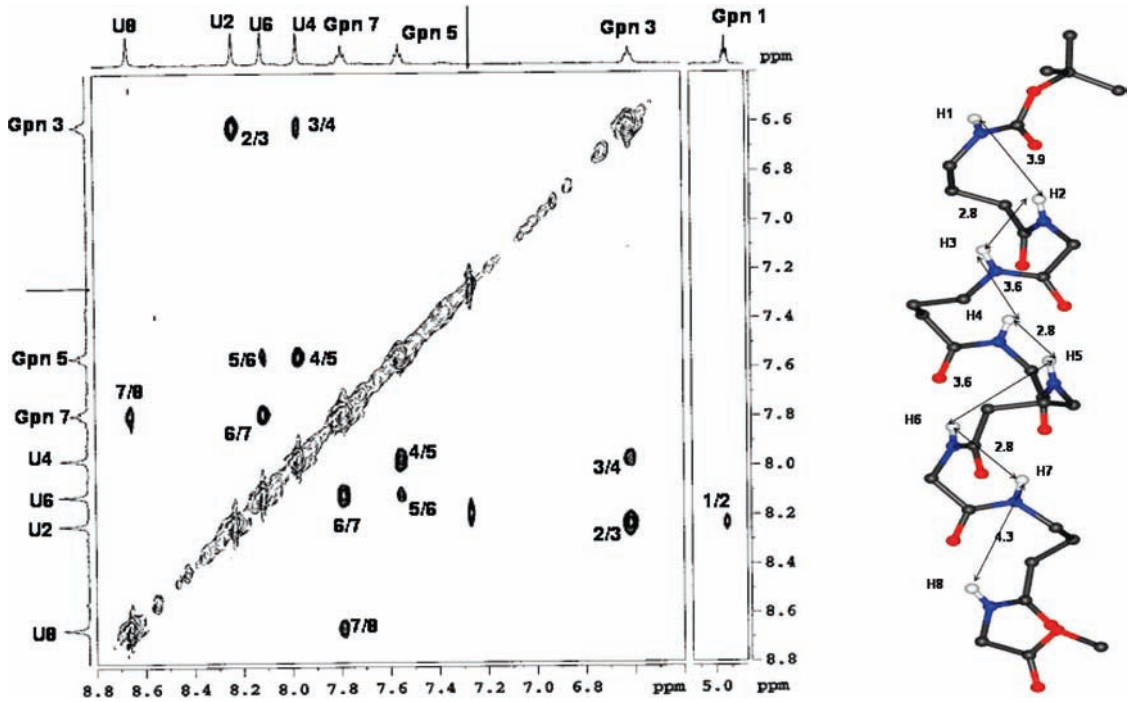

Figure 3. Partial ROESY spectrum of the peptide **1** in $CDCl_3$ at 300 K. Sequential interproton (d_{NN}) distances in the crystal are shown in the figure alongside. The average (d_{NN}) distances observed across the central Aib(2)-Aib(6) segment are d_{NN} (α) = 2.8 Å and $d_{NN}(\gamma)$ = 3.6 Å.

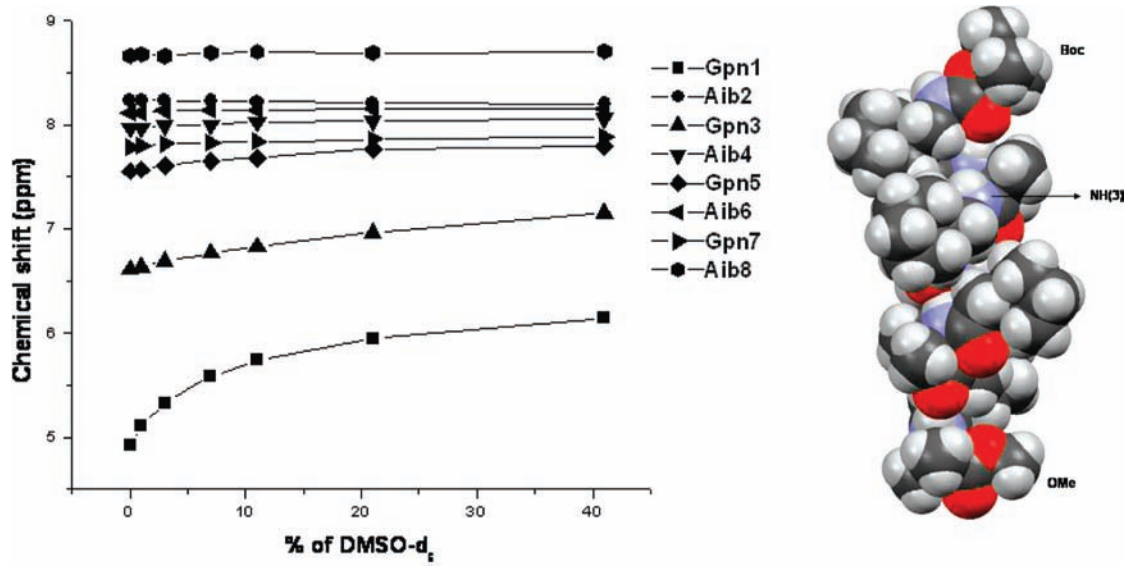

Figure 4. Plot of dependence of NH chemical shifts as a function of solvent composition ($CDCl_3$ +DMSO-d_6). A space filling model of the peptide **1** is shown alongside illustrating steric shielding of the Gpn(3) amide proton.

The 500 MHz ^{1}H NMR spectrum of octapeptide **2** in $CDCl_3$ did not yield well dispersed NH resonances. However, in CD_3OH all eight NH resonances could be identified without overlap. Sequential assignments were carried out using a combination of ROESY and TOCSY experiments. Figure 5 shows a partial ROESY spectrum highlighting the cross peaks observed between the various NH protons. A feature in this spectrum is the observation of additional peaks of low intensity which arise from a slowly exchanging conformation. Exchange cross peaks between the major and minor species observed in the ROESY spectrum establish that the minor resonances do not arise from an impurity in the sample. A notable feature of the spectrum is the wide dispersion of the aromatic proton resonances of the residues Phe(2) and Phe(7). From the partial ^{1}H spectra (Figure S8, Supporting Information) it is evident that one of the Phe(7) protons is shifted considerably upfield (6.89 δ) as a result of the ring current effect due to the proximity of the Phe(2) aromatic ring. The magnitude of the upfield shift increases as the temperature is lowered (Figure S10, Supporting Information). This upfield shift of an aromatic proton is also observed in the related octapeptide sequences which have identical strand segments,[17] suggesting that peptide **2** indeed

(17) Mahalakshmi, R.; Raghothama, S.; Balaram, P. *J. Am. Chem. Soc.* **2006**, *128*, 1125–1138.

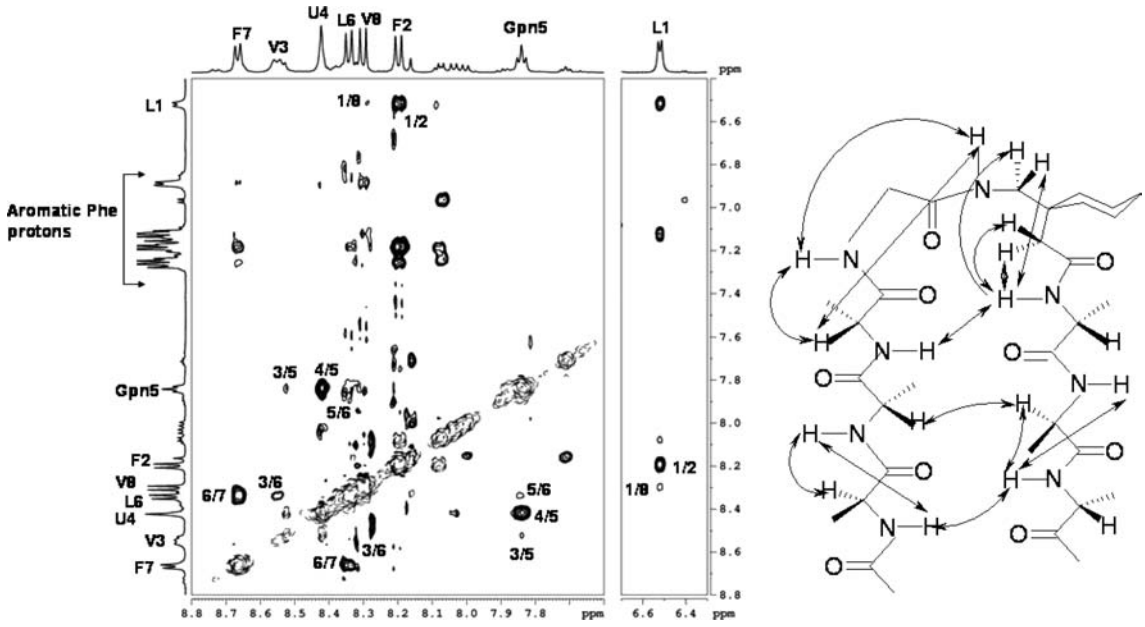

Figure 5. 500 MHz partial (NH−NH region) ROESY spectrum of the peptide **2** in CD_3OH at 300 K. All the d_{NN} NOEs observed in the spectrum are marked in the figure.

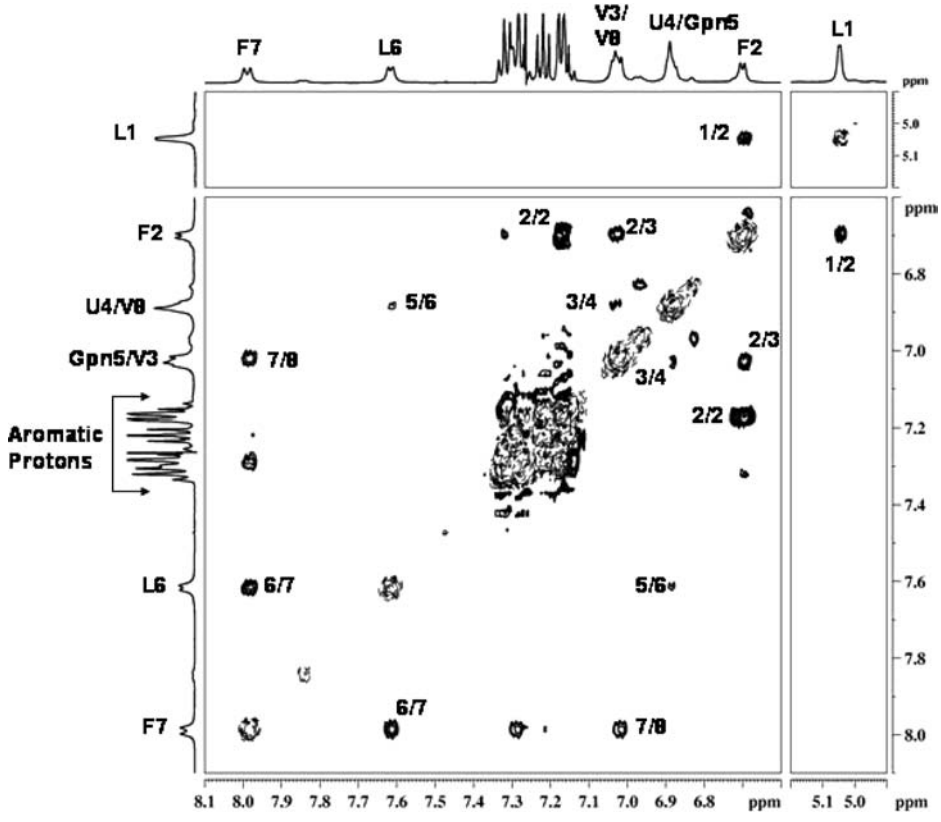

Figure 6. 500 MHz partial (NH−NH region) ROESY spectrum of the peptide **2** in $CDCl_3$ at 300 K.

folds into a hairpin structure in solution, bringing Phe(2) and Phe(7) in close proximity.

The observation of the interstrand NOEs, Val(3) NH ↔ Leu(6) NH, Leu(1) NH ↔ Val(8) NH, and Aib(4) NH ↔ Gpn(5) NH, is consistent with a hairpin conformation similar to that observed in crystals. Observation of the NOE for Val(3) NH ↔ Leu(6) NH is diagnostic for the formation of the $\alpha\gamma$ C_{12} turn at the Aib-Gpn segment. Observation of the interstrand NOE for Leu(1) NH ↔ Val(8) NH is supportive of the strand registry, even at the termini of the hairpin, and is consistent with the presence of the hydrogen bond for the Leu(1) NH···Val(8) CO, as observed in the crystal structure. Interestingly, only a very weak NOE is detected between Gpn(5) NH and Leu(6) NH. For the $\alpha\gamma$ C_{12} turn observed in the crystal structure, this interproton distance is 4.4 Å. Peptide **2** appears to predominantly populate a solution conformation in methanol

that closely resembles the hairpin structure observed in crystals. The observed backbone NOEs are summarized in Figure 5.

It must be noted that peptide **2** does show evidence for the population of multiple conformations in $CDCl_3$, as seen from the presence of low intensity peaks, selective broadening of the Val(3) NH proton, and poor dispersal of NH chemical shifts, with the Val(3)/Val(8) and Aib(4)/Gpn(5) resonances overlapping. It must be noted that the upfield shifted aromatic proton observed in the CD_3OH spectrum of peptide **2**, diagnostic of the hairpin conformation adopted by the peptide, is absent in the $CDCl_3$ spectrum. This suggests that a distinctly different conformation of peptide **2** is populated in $CDCl_3$. All the sequential d_{NN} NOEs are observed in the ROESY spectrum, except the NOE between Aib(4) NH and Gpn(5) NH protons, whose resonances overlap. The d_{NN} NOEs across the α residues are of stronger intensities than the d_{NN} NOE across the γ residue Gpn(5). This observation is diagnostic of a C_{12} helical conformation at Gpn and an α_R conformation at the α residue. Thus it may be inferred that peptide **2** adopts a helical conformation in $CDCl_3$ solution. These results suggest that the β-hairpin conformation in peptide **2** may be conformationally fragile resulting in a pronounced solvent dependence of NMR spectral properties. This is not entirely surprising as the Aib(4)-Gpn(5) $\alpha\gamma$ C_{12} turn may not be a very strong hairpin promoting structural feature. Indeed, in the conformation observed in crystals the torsion angle $\theta_2 \approx 180°$ corresponds to a *trans* orientation about the $C^{\beta}-C^{\alpha}$ bond, a feature rarely observed in the crystallographically characterized Gpn residues thus far. Presumably any energetic penalty that must be paid for adopting an unfavorable torsion angle is compensated by the cross strand hydrogen bond interactions in the folded hairpin. It should be noted that the LFV segments can also be induced to fold into a continuous helical conformation as demonstrated in the crystal structure of the octapeptide Boc-Leu-Phe-Val-Aib-βPhe-Leu-Phe-Val-OMe.[5c] Peptide **2** differs from this sequence only at position 5 where the β residue, βPhe, has been replaced by a γ residue, Gpn.

The results presented above establish that for peptide **1**, the helical conformation observed in methanol solution is completely consistent with that observed in crystals pointing to the stability of the $\alpha\gamma/\gamma\alpha$ C_{12} helical turns. For peptide **2** the NMR evidence in methanol solution favors a significant population of β-hairpin conformations, which resemble that observed in crystals. However, evidence from solvent and temperature dependence of NMR spectra has been obtained pointing to a significant heterogeneity of conformations in solution. In order for the β-hairpin registry to be maintained, the Aib-Gpn $\alpha\gamma$ C_{12} turn adopts a conformation quite distinct from that observed in the helical turns seen in peptide **1**. In $CDCl_3$ solution however, there is evidence for a helical conformation being adopted by peptide **2.** In conventional peptide sequences which are built from all α amino acid residues, the range of intramolecularly hydrogen bonded two-residue turns (β-turns) has been well characterized.[9a,18] In αα segments, type I/III turns can be propagated to give helical structures, while type II turns result in isolated chain reversals.[19] In all L-amino acid sequences found in proteins, prime turns (Type I′/Type II′) have been shown to be predominantly found as structure promoting segments in β-hairpins.[18c−e] This observation has been used extensively in the design of synthetic peptide β-hairpins incorporating centrally positioned type I′ or II′ β-turns.[6c,19,20]

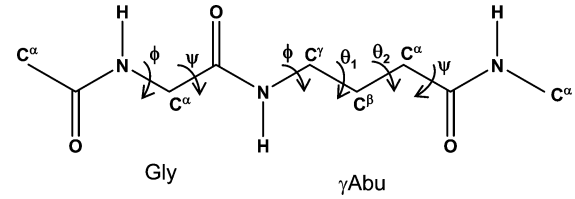

Figure 7. Definition of backbone torsion angles of the α and γ residues in the Gly-Gpn segment.

Table 3. Backbone Torsion Angles (deg) and Energy Values (kcal/mol) for Distinct Families of $\alpha\gamma$ and $\gamma\alpha$ C_{12} Hydrogen Bonded Conformations[a]

type	α-residue	γ-residue	*E* (total)
	$\alpha\gamma$ ($\theta_1 = \theta_2 = +60°$)		
I	$\phi = -60$, $\psi = -60$	$\phi = -120$, $\psi = -120$ $\theta1 = 60$, $\theta2 = 60$	−13.3
II	$\phi = -80$, $\psi = 100$	$\phi = 60$, $\psi = -120$ $\theta1 = 50$, $\theta2 = 60$	−12.2
III	$\phi = 60$, $\psi = -140$	$\phi = -140$, $\psi = -120$ $\theta1 = 55$, $\theta2 = 75$	−10.5
IV	$\phi = 80$, $\psi = -80$	$\phi = 140$, $\psi = -100$ $\theta1 = 55$, $\theta2 = 60$	−10.9
	$\alpha\gamma$ ($\theta_1 = +60°$; $\theta_2 = 180°$)		
I	$\phi = -60$, $\psi = -60$	$\phi = -100$, $\psi = 100$ $\theta1 = 80$, $\theta2 = -155$	−12.3
	$\gamma\alpha$ turns ($\theta_1 = \theta_2 = +60°$)		
I	$\phi = -100$, $\psi = -40$	$\phi = -120$, $\psi = -100$ $\theta1 = 70$, $\theta2 = 70$	−13.3

[a] The results of computational studies on other combinations of θ values are provided as Supporting Information.

To extend our understanding of the conformational possibilities for C_{12} hydrogen bonded $\alpha\gamma$ and $\gamma\alpha$ turns, we turned to theoretical modeling studies.

Theoretical Conformational Analysis. C_{12} Hydrogen Bonded Structures in $\alpha\gamma$ and $\gamma\alpha$ Sequences. The sterically allowed C_{12} hydrogen bonded conformations for the model peptide Ac-Gly-γAbu-NHMe were established using a classical grid search procedure. Rotations were performed about the backbone single bonds by varying the torsion angles ϕ, ψ for the α residue and ϕ, θ_1, θ_2, ψ for the γ residue (Figure 7).[21] Conformations which satisfy the defined limits for C═O···HN hydrogen bonds were subjected to a steric check using the outer limit distances specified by Ramachandran et al.[9b,14] Table 3 summarizes the backbone conformational angles for distinct families of C_{12} hydrogen bonded conformations for both $\alpha\gamma$ and $\gamma\alpha$ turns. Four distinct categories have been identified. The models with the lowest energies were also subjected to further minimization using the INSIGHT II module. The final energy values are provided for comparison in Table 3. The type I $\alpha\gamma$/

(18) (a) Ramachandran, G. N.; Lakshminarayanan, A. V.; Balasubramanian, R.; Tegoni, G. *Biochim. Biophys. Acta* **1970**, *221*, 165–181. (b) Lewis, P. N.; Momany, F. A.; Scheraga, H. A. *Biochim. Biophys. Acta* **1973**, *303*, 211–229. (c) Wilmot, C. M.; Thornton, J. M. *J. Mol. Biol.* **1988**, *203*, 221–232. (d) Rose, G. D.; Gierasch, L. M.; Smith, J. A. *Adv. Protein Chem.* **1985**, *37*, 1–109. (e) Sibanda, B. L.; Thornton, J. M. *Nature (London)* **1985**, *316*, 170–174. (f) Gunasekaran, K.; Gomathi, L.; Ramakrishnan, C.; Chandrasekhar, J.; Balaram, P. *J. Mol. Biol.* **1998**, *284*, 1505–1516.

(19) Venkataraman, J.; Shankaramma, S. C.; Balaram, P. *Chem. Rev.* **2001**, *101*, 3131–3152.

(20) (a) Gellman, S. H. *Curr. Opin. Chem. Biol.* **1998**, *2*, 717–725. (b) Hughes, R. M.; Waters, M. L. *Curr. Opin. Struct. Biol.* **2006**, *16*, 514–524. (c) Robinson, J. A. *Acc. Chem. Res.* **2008**, *41*, 1278–1288.

(21) For a definition of torsion angle nomenclature in backbone homologated amino acids, see: Banerjee, A.; Balaram, P. *Curr. Sci.* **1997**, *73*, 1067–1077, and ref 1b.

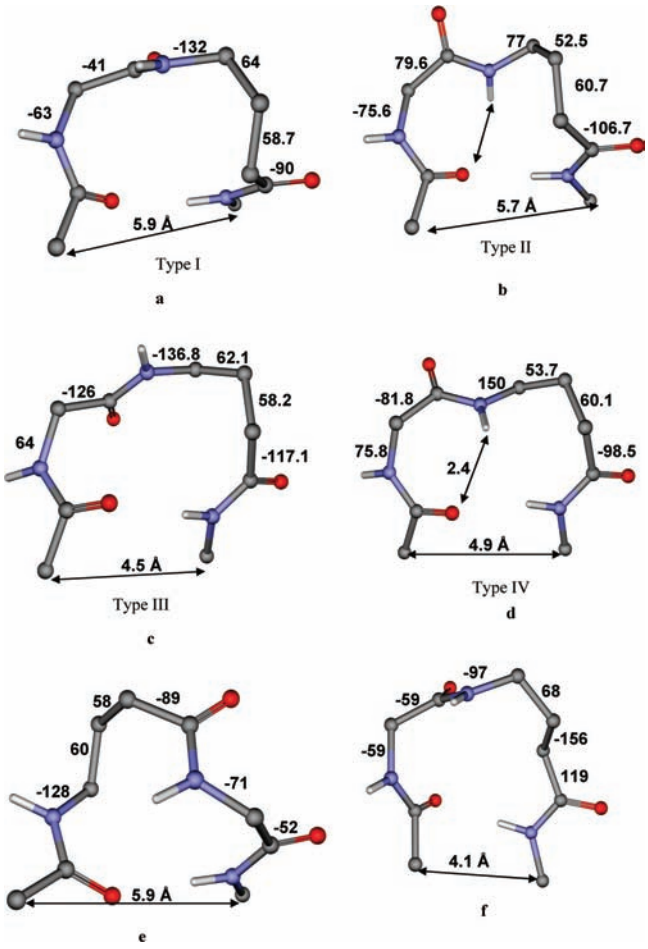

Figure 8. C_{12} hydrogen bonded turns predicted by computational studies. Structures (a)−(d) represent $\alpha\gamma$ C_{12} turns with $\theta_1 \approx \theta_2 \approx 60°$, (e) represents $\gamma\alpha$ C_{12} turns with $\theta_1 \approx \theta_2 \approx 60°$, and (f) represents $\alpha\gamma$ C_{12} turns with $\theta_1 \approx 60°$ and $\theta_2 \approx 180°$. (a), (b), (e), and (f) are experimentally characterized.

$\gamma\alpha$ turns correspond to the C_{12} turns observed in the crystal structure of peptide **1**. The torsion angles for type I $\alpha\gamma/\gamma\alpha$ C_{12} turns, which can be propagated into a C_{12}-helix established in our studies, are in good agreement with values obtained in an earlier theoretical study by Baldauf et al.[2i] A type II $\alpha\gamma$ C_{12} turn has been experimentally observed in the crystal structure of Boc-Leu-Gpn-Leu-Aib-OMe.[8e] Figure 8 illustrates the four possible $\alpha\gamma$ C_{12} turns and indicates the $C^{\alpha}(i) \leftrightarrow C^{\alpha}(i+3)$ distances (see Figure S12 of Supporting Information for the stereoviews of the C_{12} turns). The type I and type II $\alpha\gamma$ C_{12} turns are related by an approximately 180° flip of the central peptide unit, in a manner similar to the relationship between type I and type II β-turns in $\alpha\alpha$ segments, which form an internal C_{10} hydrogen bond.[9a] This process results in an approximately 180° change in ψ at the α residue and ϕ at the γ residue. The transition between the type I and type III structures involves a movement of the α residue from the right-handed helical (α_R) region of conformational space to the P_{IIR} region, which corresponds to an inversion of the classical left-handed polyproline (P_{IIL}) conformation. The type III and type IV structures are closely related, with the principal changes being in the ψ value at the α residue and the ϕ value at the γ residue. In this conformation the possibility of both C_7 (across the α residue)[22] and C_{12} hydrogen bonds is evident.[20] In all the four structures shown in Figure 8, *gauche* conformations are adopted about the $C^{\gamma}-C^{\beta}$ (θ_1) and $C^{\beta}-C^{\alpha}$ (θ_2) bonds, with the same sign for both torsion angles. When the signs for θ_1 and θ_2 are different, acceptable low energy C_{12} hydrogen bonds are not readily obtained. C_{12} hydrogen bonded turns can, however, be found for $\alpha\gamma$ segments with $\theta_1 \approx 60°$ and $\theta_2 \approx 180°$ and for $\gamma\alpha$ turns with $\theta_1 \approx 180°$ and $\theta_2 \approx 60°$. As many as six families of energetically favorable C_{12} hydrogen bonded $\alpha\gamma$ turns with $\theta_2 \approx 180°$ have been identified. These can be grouped into three pairs in which the members of a pair are related by a tilt of the central peptide unit followed by a substantial change of the ϕ value at the γ residue. In these structures, the θ_1, θ_2, and ψ values at the γ residue are almost the same for the members of a pair. One of the structures identified corresponds to the hairpin turn established in the crystal structure in peptide **2** and illustrated in Figure 8. The complete set of backbone torsion angles for these structures is provided as Supporting Information (Table S4). Similarly for $\gamma\alpha$ segments, hydrogen bonded turn structures can be identified for $\theta_1 \approx \theta_2 \approx \pm 60°$, which are observed in the C_{12} helical structures shown in Figure 8. Isolated nonhelical $\gamma\alpha$ turns did not appear as low energy structures when the α residue was not glycine. Two families of C_{12} hydrogen bonded turns with $\theta_1 = 180°$ were also identified for $\gamma\alpha$ segments, when the α residue is not glycine.

The experimental and theoretical results presented above establish that several distinct C_{12} hydrogen bonded conformations are accessible for $\alpha\gamma$ and $\gamma\alpha$ hybrid peptide segments. The crystal structures of peptides **1** and **2** provide unambiguous characterization of C_{12} hydrogen bonded turns, which can be accommodated in a continuous helical structure and at the turn segment in a peptide β-hairpin. Theoretical conformational analysis permits the definition of the backbone torsion angles that characterize energetically favorable C_{12} turns in both $\alpha\gamma$ and $\gamma\alpha$ segments. Figure 9 presents a conformational diagram which permits an understanding of the relationship between the distinct types of turn segments. The $\phi-\psi$ plot for the γ residue is presented for the *gauche*−*gauche* conformation about the $C^{\gamma}-C^{\beta}$ and $C^{\beta}-C^{\alpha}$ bonds, which is the most commonly observed conformation for the sterically constrained Gpn residue.[8] Inspection of the arrow diagram reveals the relationship between the type I and type II $\alpha\gamma$ turns. The transition requires a large change in ψ (α) and ϕ (γ), which is readily achieved by flipping the central peptide unit. Similarly, the relationship between type I and type III $\alpha\gamma$ turns and type II and type IV $\alpha\gamma$ turns is evident. The computational analysis of $\alpha\gamma$ and $\gamma\alpha$ segments reveals energetically favorable C_{12} hydrogen bonded structures, suggesting that conformational variability should be considered while interpreting solution NMR data. For peptide **2**, there is clear evidence that the structures in methanol and chloroform solutions are different. The β-hairpin conformation observed in crystals is compatible with the NMR data in CD_3OH but is not supported by the spectroscopic studies in $CDCl_3$. In developing the conformational analysis of peptide backbones containing γ residues, it is important to realize that short-range hydrogen bonded turn structures can result from several different combinations of backbone torsion angles. In the case of $\alpha\gamma$ or $\gamma\alpha$ segments, only a specific class of C_{12} hydrogen bonded turns can be propagated to give a continuous C_{12} helix, while others may facilitate hairpin chain reversals. Table 4 summarizes the

(22) For discussions of C_7 hydrogen bonds (γ-turns) in α amino acid peptides, see: (a) Nemethy, G.; Printz, M. P. *Macromolecules* **1972**, *5*, 755–758. (b) Milner-White, E. J.; Ross, B. M.; Ismail, R.; Belhady-Mostafa, K.; Poet, R. *J. Mol. Biol.* **1988**, *204*, 777–782. (c) Milner-White, E. J. *J. Mol. Biol.* **1990**, *216*, 385–397. (d) Matthews, B. W. *Macromolecules* **1972**, *5*, 818–819.

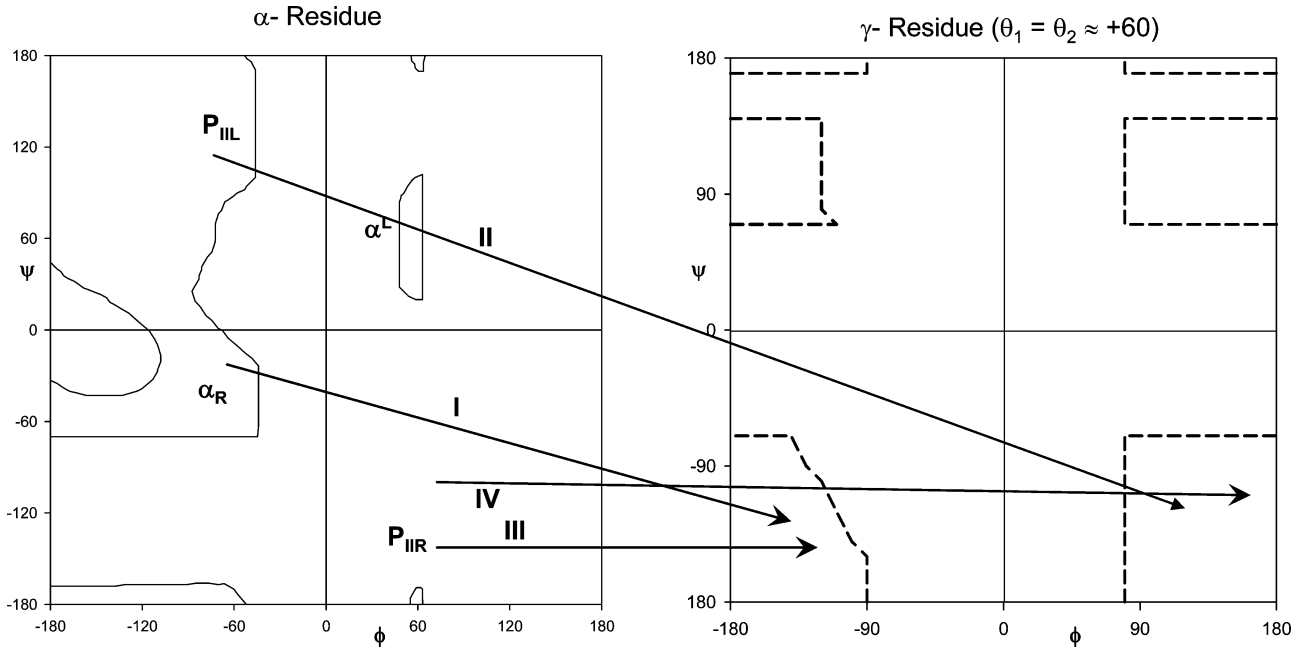

Figure 9. Conformational diagram illustrating the relationship between four distinct types of $\alpha\gamma$ C_{12} turns, in which the values of θ_1 and θ_2 for the γ residue are $+60°$.

Table 4. Backbone Torsion Angles (deg) for C_{12} Hydrogen Bonded Turns in $\alpha\gamma$ Hybrid Peptides

	α-residue		γ-residue				
type	ϕ	ψ	ϕ	θ_1	θ_2	ψ	Crystallographic observations
αγ							
C_{12} helix[a]	−63.1 (7.2)	−31.8 (13.7)	−132.1 (7.5)	53.6 (2.7)	59.9 (2.6)	−112.1 (5.3)	15
C_{12}/C_{10} helix[b]	−72.5	121.5	87.4	38.0	44.9	−129.3	1
hairpin C_{12}	−49	−41	−103	65	−167	104	1
γα							
C_{12} helix[c]	−67.1 (13.9)	−26.5 (9.9)	−117.9 (14.3)	58.4 (7.1)	61.9 (3.1)	−125.5 (18.1)	18

[a] Values are averaged over 15 experimental structures and esd's are given in parentheses. [b] In this helix the C_{12} hydrogen bond is of the type $CO_i \leftarrow HN_{i+3}$ while the C_{10} hydrogen bond is of the type $NH_i \rightarrow CO_{i+1}$. [c] In this case the experimental observations include 14 Gpn residues and 4 γAbu residues. In all the examples of $\alpha\gamma$ C_{12} turns, the γ-residue is Gpn. The values are averaged over 18 observations and the esd's are given in parentheses.

conformational parameters for crystallographically characterized C_{12} hydrogen bonded turns in $\alpha\gamma$ and $\gamma\alpha$ sequences. An understanding of the conformational choices that need to be facilitated at both the α and γ residues should aid in the rational design of specific hydrogen bonded local conformations in the $\alpha\gamma$ hybrid sequences. The use of the Gpn residues in which the torsion angles θ_1 and θ_2 are dramatically restricted because of the geminal substituents permits the experimental characterization of specific conformations. A recurring feature of our studies on gabapentin peptides is the observation of NMR evidence in solution for exchange between multiple conformational species.[7b,8c,d] In conventional α peptide sequences which lack proline residues, conformational exchange processes are generally fast on the chemical shift time scale resulting in dynamically averaged spectra. In gabapentin peptides, a transition involving movement of a Gpn residue from one position in conformational space to another (Figure 9) can involve significant barriers resulting in observation of extensive line broadening and appearance of minor resonances.

Hybrid polypeptide backbones provide a new class of backbone modified peptides which may be important in mimetic design. The experimental construction of both helical and hairpin structures accommodating $\alpha\gamma$ C_{12} turns suggests that the mimicking of conventional peptide secondary structures can be readily achieved using mixed $\alpha\gamma$ sequences. It should be of interest to experimentally establish the conformations of diverse $\alpha\gamma/\gamma\alpha$ C_{12} turns. Backbone substitution at the γ residue may be of value in limiting backbone torsion angles to specific regions of conformational space.

Acknowledgment. We thank Dr. K. Nagarajan, Hikal R&D Centre, Bangalore, for gifts of Gpn and for his continued interest. C.R. is a Senior Scientist of the Indian National Science Academy. S.C. and P.G.V. thank the Council of Scientific and Industrial Research, India, for award of Senior Research Fellowships. Research grant support was from the CSIR, India and from the Department of Biotechnology, India. The X-ray diffraction facilities are funded by the IRHPA program of the Department of Science and Technology, India and by the Indian Institute of Science, Bangalore, India.

Supporting Information Available: X-ray crystallographic information files for peptides **1** and **2** (CIF format), crystal and diffraction data and details of refinement (Table S1), NMR chemical shifts for the peptides **1** and **2** (Table S2), stereoviews and packing diagrams (Figures S1−S4) and detailed NMR

spectra (Figures S5−S10) for peptides **1** and **2**, bond lengths and bond angles of the starting model for computational studies (Figure S11), and stereoviews of the $\alpha\gamma$ hybrid turns illustrated in Figure 8 (Figure S12). X-ray crystallographic files (CIF) have also been deposited with the Cambridge Structural Database with accession numbers CCDC 7111305 (Peptide **1**) and 711306 (Peptide **2**). This material is available free of charge via the Internet at http://pubs.acs.org.

JA900618H